Acta Crystallographica Section B
Structural Science
ISSN 0108-7681

Crystal packing and melting temperatures of small oxalate esters: the role of C—H···O hydrogen bonding

Sumy Joseph, Ranganathan Sathishkumar, Sudarshan Mahapatra and Gautam R. Desiraju*

Solid State and Structural Chemistry Unit, Indian Institute of Science, Bangalore 560 012, India

Correspondence e-mail: desiraju@sscu.iisc.ernet.in

Received 29 July 2011
Accepted 14 September 2011

The simple dialkyl oxalates are generally liquids at room temperature except for dimethyl and di-*tert*-butyl oxalate which melt at 327 and 343 K. The crystal structures of diethyl, di-*iso*-propyl, di-*n*-butyl, di-*tert*-butyl and methyl ethyl oxalates were determined. The liquid esters were crystallized using the cryocrystallization technique. A comparison of the intermolecular interactions and packing features in these crystal structures was carried out. The crystal structure of dimethyl oxalate was redetermined at various temperatures. The other compounds were also studied at several temperatures in order to assess the attractive nature of the hydrogen bonds therein. A number of moderate to well defined C—H···O interactions account for the higher melting points of the two solid esters. Additionally, a diminished entropic contribution ΔS_m in di-*tert*-butyl oxalate possibly increases the melting point of this compound further.

1. Introduction

Many lower esters of simple mono- and dicarboxylic acids are liquid at room temperature. Hence only a few crystal structures of these compounds are currently available. This list includes methyl acetate (Barrow *et al.*, 1981), ethyl propionate (Shallard-Brown *et al.*, 2005*b*) and *n*-butyl acetate (Shallard-Brown *et al.*, 2005*a*). Full knowledge of the crystal structures of esters and of the intermolecular interactions therein is accordingly important.

Esters are essential components in the flavour and fragrance industry. The physical properties of esters play a role in many manufacturing strategies. On the scientific front, the importance of the study of the crystal structures of esters originates from a need to understand how intermolecular interactions manifest in the physical properties of these compounds. The preferred trajectories through which molecules approach each other to form the initial crystal nucleus are determined by directional non-bonding interactions. Molecules initially adjust and optimize themselves through the influence of hydrogen-bonding interactions which tend to operate at longer distances. These loose patterns, which are maintained by the weakly directional and electrostatic nature of hydrogen bonds, start to close pack at shorter distances with the optimization of van der Waals interactions (which operate at short range). Molecular symmetry often plays a role at this level to achieve close packing with maximum density. Interplay between directional interactions, van der Waals contribution and symmetry considerations determine the final close-packed structure with minimum free energy.

The attractive nature of the C—H···O contact was first demonstrated with a systematic analysis of neutron-based crystallographic data several years ago (Taylor & Kennard,

Table 1
Melting points (K) and boiling points (K) of dialkyl oxalates in this study.

Compound	M.p. (K)	B.p. (K)
Dimethyl oxalate	327	436
Diethyl oxalate	232	458
Di-*n*-propyl oxalate†	229	484
Di-*iso*-propyl oxalate	243	473
Di-*n*-butyl oxalate	244	514
Di-*tert*-butyl oxalate	343	502
Methyl ethyl oxalate	237	447

† Di-*n*-propyl oxalate did not give crystals under cryocrystallization conditions.

1982). Later the participation of this weak interaction in many biological molecules was shown to be quite important (Derewenda *et al.*, 1995; Jiang & Lai, 2002; Scheiner *et al.*, 2001; Wahl & Sundaralingam, 1997). The directional nature of C—H···O interactions renders them capable of being used in crystal design strategies, that is in crystal engineering (Desiraju, 1991; Desiraju & Steiner, 1998; Desiraju, 2005). Activated C—H, which is comparatively acidic, can act as a good donor for the formation of hydrogen-bonding interactions. The C···O distance *D* may be as low as 3.0 Å and the H···O distance *d* as low as 2.0 Å (Bock *et al.*, 1993). Conversely in the case of C—H···O contacts formed by unactivated C—H groups (with longer *D* values), the attractive nature of the interaction is ambiguous, and it merges with the van der Waals interaction (as manifested in its distance properties). The attractive nature of the interaction may be investigated with variable-temperature studies. True hydrogen bonds contract and become more linear as the temperature is lowered.

According to the latest definition accepted by IUPAC, 'the hydrogen bond is an attractive interaction between a hydrogen atom from a molecule or a molecular fragment *X*—H in which *X* is more electronegative than H, and an atom or a group of atoms in the same or a different molecule, in which there is evidence of bond formation' (Arunan *et al.*, 2011*a*,*b*; Desiraju, 2011). Different means are adopted to obtain such evidence of bond formation. In the case of weak C—H···O interactions, the angular dependence of the interaction is generally considered as evidence. Charge-density calculations can also give valuable information concerning bond formation. Analysis of data collected at several temperatures may also be a suitable method to confirm the bonding or attractive nature of an *X*—H···Y interaction.

The evidence that distinguishes a genuine C—H···O hydrogen bond from a van der Waals interaction becomes more indistinct as we move from activated to unactivated C—H donors. Weak C—H···O interactions formed by alkyl groups fall in the borderline region. However, the angular dependences of the interactions give a glimpse into their possible attractive nature (Steiner & Desiraju, 1998). Short C···O distances may also be a consequence of crystal packing and the C—H···O contact could even be repulsive (Seiler *et al.*, 1996). Therefore, C—H···O interactions which are at the borderline are of interest. In this context, esters are of relevance because they contain both unactivated donors and acceptors.

There are many organic compounds which are liquids at room temperature. These include solvents, low-melting solids and ionic liquids. These substances solidify at low temperatures and will often yield single crystals, but it is normally difficult to handle such crystals for X-ray study. Recent advances in cryocrystallography have made it possible to grow single crystals *in situ* at low temperatures and collect X-ray data. The crystal structures of these substances provide a valuable addition to the information bank of the crystal engineer. In a typical technique, crystallization is conducted by blowing a cold stream of N_2 onto the substance in a glass capillary mounted on the diffractometer. Some amount of microheating and annealing is often required to produce a single crystal from the microcrystalline mass that is obtained. Glass formation or vitrification is a frequent problem that prevents the formation of crystals. Almost all commercial diffractometers are equipped with a low-temperature device which makes cooling of neat liquid samples or saturated solutions feasible.

The melting point of a solid is a physical property that is determined by:

(i) the symmetry of the molecule;

(ii) intermolecular forces;

(iii) the conformational degrees of freedom of the molecule (Abramowitz & Yalkowsky, 1990).

Unlike the boiling point which is largely determined by dispersive interactions in the liquid, both enthalpic and entropic contributions play a role in the melting phenomenon. Unlike most other dialkyl oxalate esters, dimethyl oxalate DMO exists as a solid at room temperature (m.p. 327 K). As far back as 1953, Dougill and Jeffrey commented that the high melting point of DMO is on account of C—H···O hydrogen bonding. In this study we crystallized DMO and four other dialkyl oxalates that are liquid at room temperature and have studied their molecular packing in the crystal. Additionally, we investigated di-*tert*-butyl oxalate (D*t*BO) which is a solid at room temperature.

In this paper we have examined the following distinct matters:

(i) The existence of DMO and di-*tert*-butyl oxalate (D*t*BO) as solids at room temperature with melting points that are more than 100 K higher than some of their structural analogs.

(ii) The occurrence of the symmetrical diethyl oxalate (DEO) and D*t*BO molecules in general positions of a crystal that takes a centrosymmetric space group.

Additionally, we sought to perform a general analysis of the crystal structures of the lower aliphatic esters.

2. Experimental

2.1. Sample preparation and crystallization

DMO, DEO, D*t*BO, di-*n*-butyl oxalate (D*n*BO) and di-*iso*-propyl oxalate (D*i*PO) were purchased from Aldrich Chemical Co. (USA). Methyl ethyl oxalate (MEO) was

Table 2
X-ray crystallographic data for the dialkyl oxalates in this study.

Experiments were carried out with Mo $K\alpha$ radiation. Refinement was with 0 restraints. H atoms were treated by a mixture of independent and constrained refinement.

Compound	DMO	DEO	D*i*PO	D*n*BO	D*t*BO	MEO
Crystal data						
Chemical formula	$C_4H_6O_4$	$C_6H_{10}O_4$	$C_8H_{14}O_4$	$C_{10}H_{18}O_4$	$C_{10}H_{18}O_4$	$C_5H_8O_4$
M_r	118.09	146.14	174.19	202.24	202.24	132.11
Crystal system, space group	Monoclinic, $P2_1/n$	Monoclinic, $P2_1/c$	Monoclinic, $P2_1/c$	Triclinic, $P\bar{1}$	Monoclinic, $P2_1/c$	Monoclinic, $P2_1/c$
Temperature (K)	100	90	90	90	125	90
a, b, c (Å)	3.7844 (10), 11.751 (2), 6.1753 (14)	11.581 (4), 4.2812 (15), 15.282 (5)	4.2679 (17), 9.947 (4), 11.272 (5)	4.360 (2), 4.611 (2), 13.954 (7)	11.100 (2), 10.635 (2), 11.243 (2)	16.321 (8), 4.425 (2), 9.127 (4)
α, β, γ (°)	90, 104.59 (2), 90	90, 104.938 (6), 90	90, 92.444 (7), 90	81.486 (11), 81.175 (8), 81.044 (8)	90, 118.22 (3), 90	90, 95.092 (8), 90
V (Å^3)	265.76 (11)	732.1 (4)	478.1 (3)	271.6 (2)	1169.5 (5)	656.6 (5)
Z	2	4	2	1	4	4
D_x (g cm^{-3})	1.476	1.326	1.210	1.237	1.149	1.337
μ (mm^{-1})	0.135	0.11	0.10	0.09	0.09	0.12
Crystal size (mm^3)	0.17 × 0.2 × 0.25	0.35 × 0.50 × 0.50	0.35 × 0.50 × 0.50	0.35 × 0.50 × 0.50	0.35 × 0.35 × 0.50	0.35 × 0.50 × 0.50
Data collection						
Diffractometer	Oxford Xcalibur, Eos(Nova) CCD detector	Bruker SMART CCD area detector	Bruker SMART CCD area detector	Bruker SMART CCD area detector	Rigaku Mercury-375R (2 × 2 bin mode)	Bruker SMART CCD area detector
Absorption correction	–	–	–	Multi-scan (*SADABS*; Sheldrick, 2008)	Multi-scan (Jacobson, 1998)	Multi-scan (*SADABS*; Sheldrick, 2008)
T_{min}, T_{max}	–	–	–	0.954, 0.968	0.957, 0.970	0.944, 0.960
No. of measured, independent and observed [$> 2\sigma(I)$] reflections	2188, 489, 394	6617, 1345, 817	4124, 864, 705	2826, 1204, 1046	10 238, 2149, 1960	5453, 1207, 918
R_{int}	0.042	0.058	0.048	0.045	0.056	0.054
$(\sin\theta/\lambda)_{max}$ (Å^{-1})	0.604	0.604	0.604	0.649	0.604	0.604
Refinement						
R_1 [$I > 2\sigma(I)$], wR_2, S	0.048, 0.126, 1.17	0.049, 0.121, 1.07	0.051, 0.133, 1.11	0.095, 0.252, 1.26	0.037, 0.097, 1.08	0.093, 0.280, 1.30
No. of reflections	489	1345	864	1204	2149	1207
No. of parameters	49	131	83	100	199	114
$\Delta\rho_{max}$, $\Delta\rho_{min}$ (e Å^{-3})	0.27, −0.23	0.21, −0.18	0.27, −0.22	0.76, −0.32	0.19, −0.19	0.49, −0.45
CCDC No.	835069	829931	829933	836365	835074	836433

prepared from the monopotassium salt of monoethyl oxalate as follows. An equimolar mixture of DEO and potassium acetate was refluxed at 363 K in the presence of 0.1 *M* equivalents each of EtOH and water. The white colored crystalline potassium ethyl oxalate that was obtained was acidified with dilute HCl to give monoethyl oxalate. This was extracted with ether and treated with an ethereal solution of diazomethane generated *in situ* from nitrosomethylurea to give MEO.

DMO single crystals were grown from a melt under vacuum. The crystals are soft and air sensitive. Therefore, they were sealed in a Lindemann capillary tube as soon as they were taken out of the vacuum. Single crystals of D*t*BO crystals were obtained from the commercially available sample bottle. Although its melting point is high, D*t*BO is highly volatile in air, and therefore the crystal was sealed in a capillary.

2.2. Cryocrystallization

DEO, D*i*PO, D*n*BO and MEO were crystallized employing cryocrystallization conditions. In the case of D*n*PO, we could not crystallize the sample due to glass formation in the capillary column.

Differential scanning calorimetry (DSC) was carried out initially for the above-mentioned liquid oxalates to optimize the crystallization temperature. A Lindemann glass capillary (0.5 mm diameter) was almost fully filled with the liquid oxalate and flame-sealed at both ends; the capillary was then mounted on the goniometer head of a Bruker AXS single-crystal X-ray diffractometer equipped with a SMART APEX CCD area detector. The capillary was aligned to the X-ray beam under an OXFORD N_2 cryosystem using the video setting in the computer, and cooled to the required tempera-

Table 3
Geometrical parameters of C—H···O hydrogen bonds in the other alkyl oxalates at different temperatures.

C—H distances are normalized.

Compound	Temperature	H-bridge	d (H···A) (Å)	D (X···A) (Å)	θ (X—H···A) (°)
DEO	170	C2—H2*B*···O1	2.59	3.667 (4)	175
		C5—H5*B*···O2	2.59	3.670 (4)	178
		C6—H6*A*···O1	2.72	3.704 (5)	152
	90	C2—H2*B*···O1	2.57	3.648 (3)	174
		C5—H5*B*···O2	2.57	3.646 (3)	176
		C6—H6*A*···O1	2.70	3.655 (4)	147
D*i*PO	210	C2—H2···O2	2.71	3.660 (3)	146
		C3—H3*B*···O1	2.76	3.747 (4)	152
		C4—H4*A*···O1	2.64	3.548 (3)	141
		C4—H4*C*···O1	2.62	3.619 (3)	152
	90	C2—H2···O2	2.62	3.592 (3)	149
		C3—H3*B*···O1	2.70	3.659 (4)	147
		C4—H4*A*···O1	2.59	3.502 (4)	141
		C4—H4*C*···O1	2.59	3.558 (4)	149
D*n*BO	210	C2—H2*A*···O1	2.64	3.398 (8)	127
		C2—H2*B*···O2	2.82	3.706 (8)	139
		C3—H3*A*···O1	2.75	3.589 (8)	134
	90	C2—H2*A*···O1	2.49	3.377 (5)	138
		C2—H2*B*···O2	2.70	3.477 (5)	129
		C3—H3*A*···O1	2.60	3.391 (5)	130
MEO	170	C1—H1*A*···O1	2.61	3.482 (8)	137
		C1—H1*A*···O3	2.58	3.619 (8)	161
		C1—H1*C*···O3	2.65	3.508 (8)	135
		C4—H4*B*···O4	2.64	3.726 (9)	179
	90	C1—H1*A*···O1	2.70	3.459 (7)	127
		C1—H1*A*···O3	2.52	3.587 (6)	170
		C1—H1*C*···O3	2.59	3.465 (7)	137
		C4—H4*B*···O4	2.61	3.692 (7)	176

ture at a ramping rate of 200 K h^{-1} using the cryosystem program. The temperature at which the N_2 cryostream has to be maintained was determined based on DSC. The crystallization of liquid was checked by holding the temperature and taking still pictures at 5–10 K intervals. Uniformity in temperature on the capillary was maintained by rotating the capillary with the same cooling rate. A polycrystalline mass formed at this stage. In order to obtain a good quality single crystal, the crystal column was zone refined (annealed) by adjusting the cryo head with three degrees of freedom. At each and every stage of zone refinement, still and rotation pictures were taken to assure the quality of diffraction. In this way, good quality crystals were obtained.

The rotation photographs for the crystal prior to data collection were checked to ascertain the quality of the diffraction spots. The temperature was allowed to stabilize for half an hour after which 180 frames of data were collected by performing an ω scan width of -1° with the 2θ fixed at -25°. The obtained frames were processed using *SMART* (Bruker 2004), and the spots were analyzed using the *RLATT* (Bruker 2004, Version 30) program at high accuracy to determine the unit-cell dimensions. Data were collected on four sets of 606 frames with $2\theta = -25^\circ$ and with φ values of 0, 90, 180 and 270°. The crystal structure was solved using *SIR*92 and *SHELXL* (Sheldrick, 2008). All H atoms were located from difference maps, normalized at 1.08 Å and refined isotropically. For all samples, the data were collected at two different temperatures in order to verify the attractive nature of the interaction.

Individual details are now narrated:

(i) DEO was crystallized in the cooling cycle at 170 K. The polycrystalline DEO formed immediately after the temperature reached 170 K. Final zone refinement to a single crystalline domain took 5 h. Data were of good quality. Data were collected at 170 and 90 K.

(ii) D*i*PO: The polycrystalline sample formed quite spontaneously at 210 K during the cooling cycle. The transition from a polycrystalline solid to a single crystal by zone refinement took 5 h. Data were collected at 210 and 90 K.

(iii) D*n*BO was crystallized in the cooling cycle at 210 K. The zone refinement of the polycrystalline sample to a single crystal took nearly 12 h. This process was tedious owing to the formation of a glassy phase on the edges of the polycrystalline mass. The presence of the long alkyl end chain possibly results in a disordered crystal and a high R value. However, a good quality crystal could be obtained after repeated trials. The disorder decreased as the temperature was lowered to 90 K. Data were collected at 210 and 90 K.

(iv) MEO was crystallized in the cooling cycle at 170 K. Unlike the other samples, the crystal quality did not improve after repeated attempts of local heating/cooling. The best data obtained at 170 K was with an R factor of 10.8. The data quality improved with a lowering of the temperature to 90 K. Data were collected at 170 and 90 K.

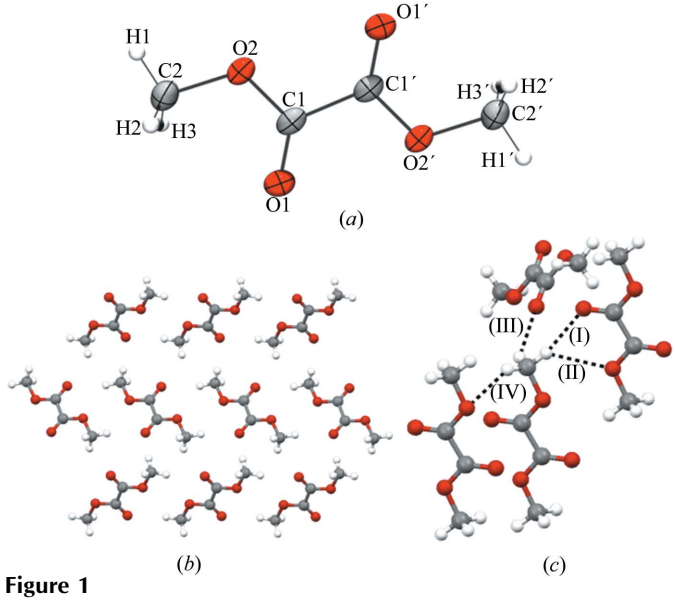

Figure 1
Dimethyl oxalate, DMO: (*a*) single molecule *ORTEP* drawing at the 50% probability level; (*b*) packing of molecules; (*c*) C—H···O interactions.

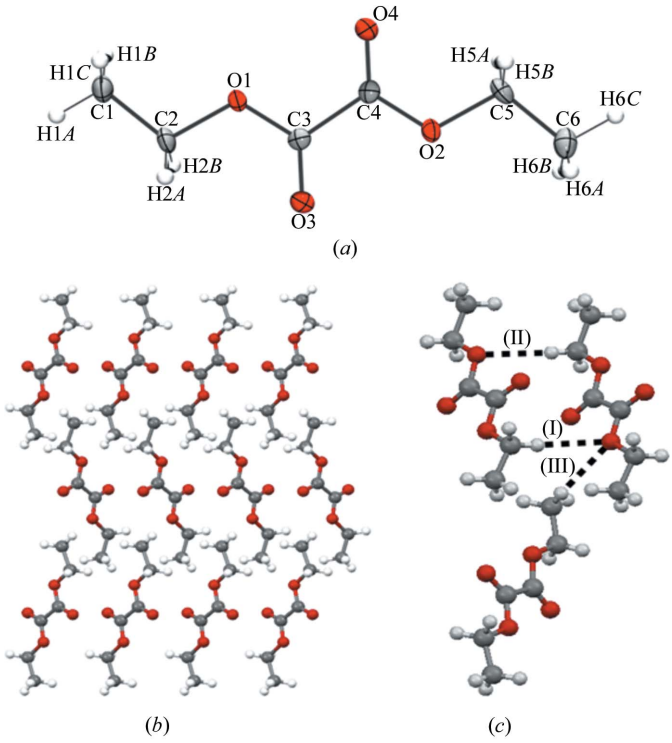

Figure 2
Diethyl oxalate, DEO: (*a*) single molecule *ORTEP* drawing at the 50% probability level; (*b*) view down the *a* axis; (*c*) three intermolecular C–H···O interactions observed.

2.3. Single-crystal X-ray diffraction

Single-crystal data for the DMO crystal were collected on an Oxford single-crystal X-ray diffractometer (Microsource: Mova; Detector: Eos) with a liquid nitrogen cooling and heating facility. Data were collected at various temperatures by cooling the crystal to a low temperature (323–100 K) and the structures were solved with direct methods (Altomare *et al.*, 1993; Oxford Diffraction Ltd, 2007). Data were collected for D*t*BO on a Rigaku Mercury 375R/M CCD (XtaLAB mini) diffractometer using graphite-monochromated Mo $K\alpha$ radiation, equipped with a Rigaku low-temperature gas spray cooler. Data were collected in the cooling cycle at various temperatures (250–125 K) and processed with the Rigaku *CrystalClear* software (Rigaku Corporation, 2007; Pflugrath, 1999). Structure solution and refinements were performed using *SHELX*97 (Sheldrick, 2008) and the *WinGX* suite (Farrugia, 1999).

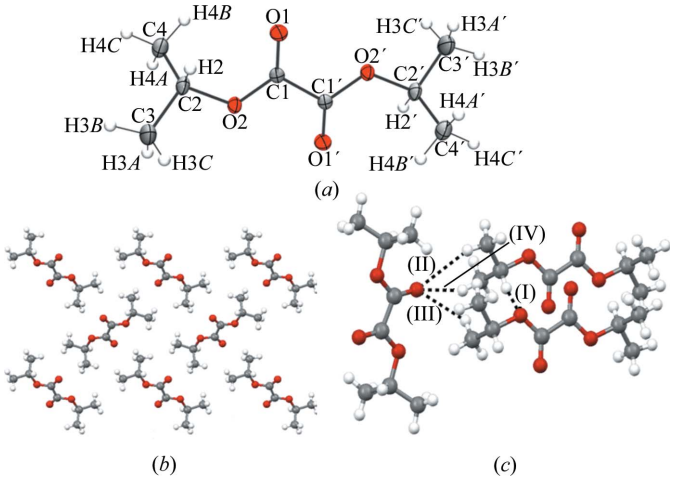

Figure 3
Di-*iso*-propyl oxalate, D*i*PO: (*a*) single molecule *ORTEP* drawing at the 50% probability level; (*b*) view down the *a* axis; (*c*) four intermolecular C—H···O interactions observed.

3. Results and discussion

All the dialkyl oxalates in this study exist as liquids at room temperature except DMO and D*t*BO. An examination of the melting points of the esters (Scheme 1) we studied shows a range of ∼115 K (Table 1). This variation in melting points among closely related compounds can be studied in the light of how the molecules are packed in the crystal lattice and through an understanding of the intermolecular interactions therein. The X-ray crystallographic data is given in Table 2.[1] The first report on the crystal structure of DMO (Dougill & Jeffrey, 1953) attributed the existence of DMO in the solid state to the formation of a number of C—H···O bonds as a result of the molecular environment in which each of the methyl and carbonyl oxygens are situated. They explained hydrogen-bond formation as polarization bonding. This paper was one of the earliest reports of C—H···O hydrogen bonding in the solid state. It is therefore of historical interest. Now the question is why all the other esters cannot accommodate such a bonding interaction environment in the crystal lattice. For this we have studied a number of dialkyl oxalates including the unsymmetrical ester MEO.

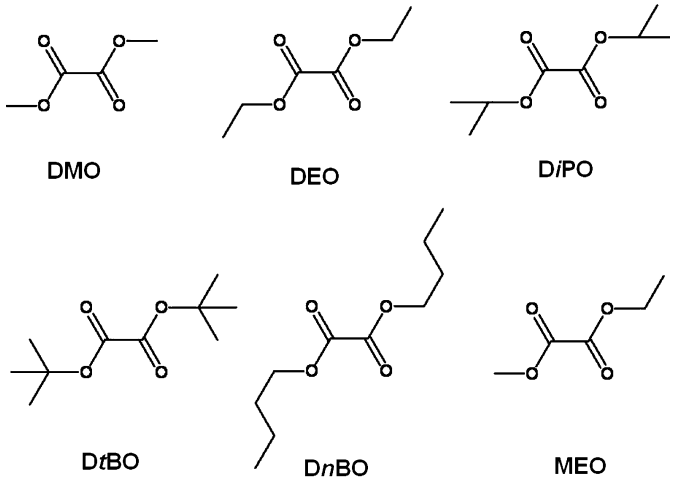

Scheme 1

3.1. Dimethyl oxalate (DMO)

The structure (Dougill & Jeffrey, 1953) was further analysed (Jones *et al.*, 1989) for the determination of the C-13 chemical

[1] Supplementary data for this paper are available from the IUCr electronic archives (Reference: OG5050). Services for accessing these data are described at the back of the journal.

Table 4
X-ray crystallographic data for DMO as a function of temperature.

For all structures: $C_4H_6O_4$, M_r = 118.09, monoclinic, $P2_1/n$, Z = 2. Experiments were carried out with Mo $K\alpha$ radiation using an Oxford Xcalibur, Eos(Nova) CCD detector diffractometer. Refinement was on 49 parameters with 0 restraints. H atoms were treated by a mixture of independent and constrained refinement.

Temperature T (K)	323	273	200	150	100
Crystal data					
a, b, c (Å)	3.9101 (19), 11.907 (5), 6.221 (3)	3.873 (2), 11.875 (4), 6.205 (2)	3.851 (2), 11.840 (6), 6.227 (3)	3.8083 (15), 11.742 (4), 6.1664 (18)	3.7844 (10), 11.751 (2), 6.1753 (14)
β (°)	103.10 (5)	103.37 (4)	104.31 (5)	104.06 (3)	104.59 (2)
V (Å^3)	282.1 (2)	277.7 (2)	275.1 (2)	267.48 (16)	265.76 (11)
D_x (Mg m^{-3})	1.390	1.412	1.426	1.466	1.476
μ (mm^{-1})	0.13	0.13	0.13	0.13	0.14
Crystal size (mm)	0.25 × 0.20 × 0.17	0.25 × 0.20 × 0.17	0.25 × 0.20 × 0.17	0.25 × 0.20 × 0.17	0.25 × 0.20 × 0.17
Data collection					
Absorption correction	–	–	–	–	
No. of measured, independent and observed [$> 2\sigma(I)$] reflections	2421, 524, 275	3942, 515, 319	4697, 508, 390	2457, 491, 372	2188, 489, 394
R_{int}	0.052	0.063	0.074	0.046	0.0.42
$(\sin\theta/\lambda)_{max}$ (Å^{-1})	0.604	0.604	0.604	0.604	0.604
Refinement					
R_1 [$I > 2\sigma(I)$], wR_2, S	0.052, 0.162, 0.97	0.055, 0.161, 1.03	0.056, 0.153, 1.09	0.048, 0.124, 1.13	0.048, 0.126, 1.17
No. of reflections	524	515	508	491	489
$\Delta\rho_{max}$, $\Delta\rho_{min}$ (e Å^{-3})	0.14, −0.13	0.21, −0.17	0.21, −0.22	0.25, −0.21	0.27, −0.23
CCDC No.	835073	835072	835071	835070	835069

shielding tensors of the carbonyl carbon. We have redetermined the structure at several temperatures. Fig. 1(*b*) shows the packing diagram down the *a* axis. The methyl-group H atoms are polarized by adjacent O atoms and each of them is C—H···O hydrogen bonded, with one being bifurcated. There are therefore four C—H···O hydrogen bonds [labelled (I), (II), (III) and (IV) in Fig. 1*c*] with *D* distances 3.559 (4), 3.553 (5), 3.577 (5) and 3.614 (5) Å at 273 K. These interactions are of moderate strength. The molecules are planar and are packed so that adjacent molecular planes are inclined at an angle of 69°.

3.1.1. Diethyl oxalate (DEO). DEO crystallizes in the space group $P2_1/c$ with Z = 4. Fig. 2(*b*) shows the packing diagram down the *a* axis. In spite of being centrosymmetric, the molecule lies on a general position rather than on a crystallographic inversion center. There does not seem to be any obvious reason for this such as synthon symmetry (Banerjee *et al.*, 2003). Three weak intermolecular C—H···O interactions with C···O distances 3.667 (4), 3.670 (4) and 3.704 (5) Å at 170 K may be identified and are designated (I), (II) and (III) in Fig. 2(*c*). Unusually, carbonyl oxygen is not involved – all three hydrogen bonds are to alkoxy oxygen. It is useful to examine low-temperature data to study these hydrogen bonds because both donors and acceptors are very weak, especially in interaction (III). The intermolecular C—H···O interaction *D* values in DEO are shown in Table 3. As the temperature decreases, the *D* value also decreases showing the attractive nature of the interactions.

3.1.2. Di-*iso*-propyl oxalate (D*i*PO). D*i*PO crystallizes in the space group $P2_1/c$ with Z' = 0.5. The molecules are planar. There are four weak C—H···O interactions present and at 210 K their *D* values are 3.660 (3), 3.747 (4), 3.548 (3) and 3.619 (3) Å (Fig. 3*c*). Three of these interactions are between methyl H atoms and carbonyl oxygen. The fourth one is from an activated methine hydrogen to alkoxyl oxygen. The molecules are packed similarly to DMO and are inclined at an angle of 40° to one another (Fig. 3*b*) but the C—H···O bonds are generally longer. These contacts are still attractive because their lengths decrease with a decrease in temperature.

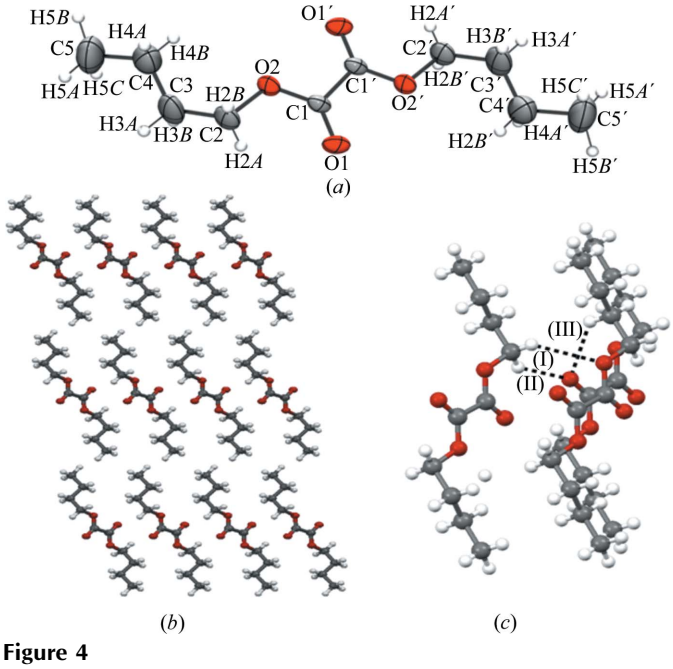

Figure 4
Di-*n*-butyl oxalate, D*n*BO: (*a*) single molecule *ORTEP* drawing at the 50% probability level; (*b*) view down the *a* axis; (*c*) three intermolecular C—H···O interactions observed.

Table 5
X-ray crystallographic data for D*t*BO oxalate as a function of temperature.

For all structures: $C_{10}H_{18}O_4$, M_r = 202.24, monoclinic, $P2_1/c$, Z = 4. Experiments were carried out with Mo $K\alpha$ radiation using a Rigaku Mercury375R (2 × 2 bin mode) diffractometer. Absorption was corrected for by multi-scan methods (Jacobson, 1998). Refinement was on 199 parameters with 0 restraints. H atoms were treated by a mixture of independent and constrained refinement.

Temperature T (K)	250	225	200	175	150	125
Crystal data						
a, b, c (Å)	11.197 (2), 10.778 (2), 11.454 (2)	11.183 (2), 10.752 (2), 11.405 (2)	11.163 (2), 10.720 (2), 11.359 (2)	11.138 (2), 10.686 (2), 11.324 (2)	11.120 (2), 10.650 (2), 11.277 (2)	11.100 (2), 10.635 (2), 11.243 (2)
β (°)	119.23 (3)	118.95 (3)	118.75 (3)	118.61 (3)	118.35 (3)	118.22 (3)
V (Å^3)	1206.3 (5)	1200.0 (5)	1191.7 (5)	1183.2 (5)	1175.3 (5)	1169.5 (5)
D_x (Mg m^{-3})	1.114	1.120	1.127	1.135	1.143	1.149
μ (mm^{-1})	0.09	0.09	0.09	0.09	0.09	0.09
Crystal size (mm)	0.50 × 0.35 × 0.35	0.50 × 0.35 × 0.35	0.50 × 0.35 × 0.35	0.50 × 0.35 × 0.35	0.50 × 0.35 × 0.35	0.50 × 0.35 × 0.35
Data collection						
T_{min}, T_{max}	0.959, 0.971	0.959, 0.971	0.958, 0.970	0.958, 0.970	0.958, 0.970	0.957, 0.970
No. of measured, independent and observed [$> 2\sigma(I)$] reflections	10 513, 2209, 1879	10 476, 2199, 1919	10 415, 2186, 1936	10 363, 2174, 1948	10 287, 2157, 1947	10 238, 2149, 1960
R_{int}	0.057	0.059	0.054	0.054	0.054	0.056
$(\sin\theta/\lambda)_{max}$ (Å^{-1})	0.604	0.604	0.604	0.604	0.604	0.604
Refinement						
R_1 [$I > 2\sigma(I)$], wR_2, S	0.048, 0.133, 1.06	0.046, 0.122, 1.08	0.041, 0.111, 1.07	0.039, 0.100, 1.10	0.038, 0.099, 1.05	0.037, 0.097, 1.08
No. of reflections	2209	2199	2186	2174	2157	2149
$\Delta\rho_{max}$, $\Delta\rho_{min}$ (e Å^{-3})	0.25, −0.17	0.23, −0.18	0.21, −0.17	0.21, −0.20	0.22, −0.20	0.19, −0.19
CCDC No.	835079	835078	835077	835076	835075	835074

3.1.3. Di-*n*-butyl oxalate (D*n*BO). The increase in chain length becomes manifested in the molecular packing. The molecules pack in a linear fashion instead of the inclined arrangement seen in DMO, DEO, D*i*PO and D*t*BO (Fig. 4*b*). This could be an example of the hydrophobic effect which commonly begins to manifest itself when a linear C_4 chain is present. The carbonyl oxygen accepts hydrogen bonds from both activated and unactivated methylene H atoms in a bifurcated manner [interactions (II) and (III)]. A third hydrogen bond exists between an alkoxyl oxygen and an activated methylene hydrogen [interaction (I)]. The Z' value is 0.5 with the molecule situated on an inversion center. Upon decreasing the temperature, the d and D values decreases. This shortening with temperature is characteristic of genuine hydrogen bonds.

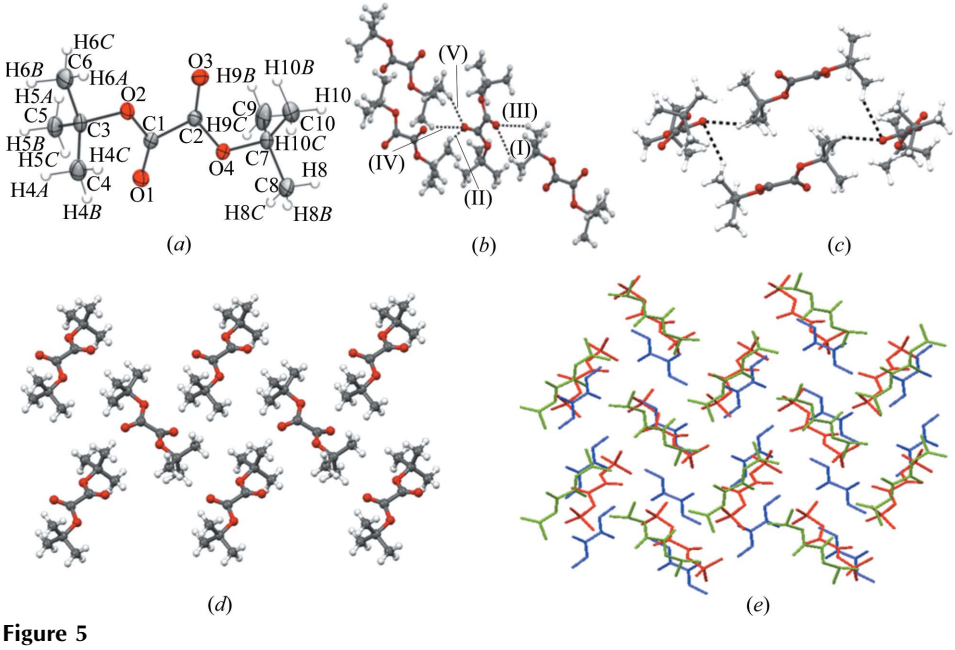

Figure 5
Di-*tert*-butyl oxalate, D*t*BO: (*a*) single molecule *ORTEP* drawing at the 50% level; (*b*) five intermolecular C—H···O interactions observed; (*c*) tetramer synthon, formed by C—H···O hydrogen bonds, that lies on the inversion center; (*d*) view down the *a* axis; (*e*) a merged figure showing the molecular packing similarity in DMO (blue), D*i*PO (green) and D*t*BO (red).

3.1.4. Di-*tert*-butyl oxalate (D*t*BO). D*t*BO takes the space group $P2_1/c$. The molecules have a typical monoclinic packing. Five different C—H···O hydrogen-bonding interactions are observed. Four are bifurcated and within the typical range with distances of 3.553 (3), 3.610 (3), 3.551 (3) and 3.509 (4) Å at 250 K [see interactions (I), (III), (IV) and (V) in Fig. 5*b*]. A network of these interactions constitutes the *ac* plane (Fig. 5*d*). In the third direction there is another C—H···O interaction of 3.610 (3) Å [interaction (II), Fig. 5*b*]. Only the carbonyl O atom is involved in all the interactions. Even though D*t*BO is a symmetrical molecule it crystallizes with Z'

Table 6
Geometrical parameters of C—H···O hydrogen bonds in DMO and D*t*BO at different temperatures.

C—H distances are normalized.

Compound	Temperature	H-bridge	d (H···A) (Å)	D (X···A) (Å)	θ (X—H···A) (°)
DMO	323	C2—H1···O1	2.51	3.583 (5)	172
		C2—H1···O2	2.82	3.578 (5)	127
		C2—H2···O1	2.83	3.596 (6)	128
		C2—H3···O2	2.69	3.652 (5)	148
	273	C2—H1···O1	2.50	3.559 (4)	166
		C2—H1···O2	2.74	3.553 (5)	132
		C2—H2···O1	2.83	3.577 (5)	126
		C2—H3···O2	2.63	3.614 (5)	151
	200	C2—H1···O1	2.50	3.565 (4)	167
		C2—H1···O2	2.74	3.535 (4)	130
		C2—H2···O1	2.70	3.549 (4)	135
		C2—H3···O2	2.63	3.612 (4)	150
	150	C2—H1···O1	2.46	3.524 (3)	166
		C2—H1···O2	2.67	3.485 (3)	131
		C2—H2···O1	2.68	3.507 (3)	133
		C2—H3···O2	2.58	3.570 (3)	151
	100	C2—H1···O1	2.47	3.525 (3)	165
		C2—H1···O2	2.66	3.469 (3)	131
		C2—H2···O1	2.61	3.498 (3)	139
		C2—H3···O2	2.58	3.562 (4)	150
D*t*BO	250	C4—H4*A*···O3	2.56	3.553 (3)	151
		C4—H4*C*···O1	2.64	3.523 (3)	138
		C6—H6*B*···O3	2.67	3.610 (3)	145
		C8—H8*A*···O1	2.59	3.551 (3)	147
		C9—H9*A*···O1	2.55	3.509 (4)	147
	225	C4—H4*A*···O3	2.56	3.549 (3)	151
		Cs4—H4*C*···O1	2.65	3.506 (3)	136
		C6—H6*B*···O3	2.66	3.596 (3)	145
		C8—H8*A*···O1	2.59	3.545 (3)	147
		C9—H9*A*···O1	2.53	3.502 (3)	149
	200	C4—H4*A*···O3	2.55	3.541 (2)	151
		C4—H4*C*···O1	2.63	3.493 (2)	136
		C6—H6*B*···O3	2.62	3.582 (2)	148
		C8—H8*A*···O1	2.57	3.535 (3)	147
		C9—H9*A*···O1	2.51	3.494 (3)	151
	175	C4—H4*A*···O3	2.55	3.531 (2)	151
		C4—H4*C*···O1	2.60	3.481 (2)	138
		C6—H6*B*···O3	2.62	3.568 (2)	146
		C8—H8*A*···O1	2.56	3.526 (2)	148
		C9—H9*A*···O1	2.49	3.484 (3)	152
	150	C4—H4*A*···O3	2.55	3.524 (2)	150
		C4—H4*C*···O1	2.59	3.470 (2)	138
		C6—H6*B*···O3	2.60	3.5544 (19)	146
		C8—H8*A*···O1	2.56	3.515 (2)	147
		C9—H9*A*···O1	2.49	3.475 (2)	151
	125	C4—H4*A*···O3	2.53	3.5144 (19)	150
		C4—H4*C*···O1	2.58	3.4572 (19)	138
		C6—H6*B*···O3	2.59	3.5414 (18)	146
		C8—H8*A*···O1	2.55	3.509 (2)	148
		C9—H9*A*···O1	2.48	3.467 (2)	152

= 1. This behaviour is similar to that of DEO. However, unlike DEO it is possible to rationalize the location of a molecule on a general position in that a robust supramolecular synthon (Fig. 5*c*) is located on the inversion center (Banerjee *et al.*, 2003). Variable-temperature XRD studies show that as the temperature decreases, the C—H···O distances become shorter which is indicative of an attractive interaction.

It is noteworthy to mention the molecular packing similarity exhibited by DMO, D*i*PO and D*t*BO. The molecules are close packed with a glide between the adjacent molecules resulting in a typical monoclinic packing with angles in the range 40–70° between adjacent molecular planes. The similarity in molecular packing is more clearly manifested in a merged figure of these three structures (Fig. 5*e*).

3.1.5. Methyl ethyl oxalate (MEO). The behavior of an unsymmetrical ester is studied by examining the packing of molecules in MEO. MEO crystallizes in the monoclinic crystal system (space group $P2_1/c$) with $Z' = 1$. Among the four weak hydrogen bonds observed, two [(II) and (III)] are between activated methyl H and carbonyl O atoms. A view down the c axis (Fig. 6*b*) gives a further understanding of the packing. The structure is layer-like with the length of the molecule corresponding to the layer thickness. The methyl–methyl (M–M) separation is closer (partial interlocking of layers) than the ethyl–ethyl (E–E) separation so that there is a larger interlayer region at the ethyl–ethyl interface.

3.1.6. Variable-temperature data analysis. A detailed analysis of variable-temperature data was carried out for the two solid compounds DMO and D*t*BO. The X-ray crystallographic data are given in Tables 4 and 5. Geometrical parameters of C–H···O hydrogen bonds are given in Table 6. As mentioned by Dougill and Jeffrey in their paper, there are four weak hydrogen bonds in DMO; two are to carbonyl oxygen and the other two are to alkoxy oxygen. The value of d, D and θ are compared for different temperatures. With decreasing temperature the values of d and D decrease indicating an attractive interaction. The C···O (D) *versus* temperature plot for DMO and D*t*BO supports the attractive nature of the interaction (Fig. 7).

3.2. Melting temperatures of small aliphatic esters

The melting temperature T_m of a molecular solid is defined as $\Delta H_m/\Delta S_m$, where ΔH_m and ΔS_m are the enthalpy and entropy of fusion. A higher melting point is obtained when the former increases and/or the latter decreases. In effect the melting point is determined by:

(i) the intermolecular interactions which affect the ΔH_m term;

(ii) the molecular symmetry;

(iii) the conformational freedom, both of which affect the ΔS_m term.

A list of melting points and boiling points of the compounds studied are given in Table 1. Among the different homologues of DMO studied here, a comparison of intermolecular hydrogen bonds can be made by examining the number and strength of C—H···O interactions.

It was suggested that in DMO the existence of the compound in the solid state compared with its other functional

analogues is due to a larger number of hydrogen bonds (Dougill & Jeffrey, 1953). The donor efficiency of the methyl group hydrogen in DMO is augmented by the presence of neighboring carbonyl O atoms. This leads to the formation of four different attractive hydrogen bonds. The attractive nature is now confirmed by our variable-temperature study. As the temperature decreases an authentic hydrogen bond shows a decrease in *D* value. It is obvious from Table 6 that DMO and especially D*t*BO have a large number of good hydrogen bonds. Although D*i*PO and MEO also exhibit hydrogen-bonding interactions, these are weak (long) when compared with DMO and D*t*BO. When the methyl group is substituted with other alkyl groups the gain in conformational freedom upon melting increases due to the flexible nature of the alkyl groups. Therefore, the ΔS_m term increases for the higher dialkyl oxalates DEO, MEO, D*i*PO and D*n*BO; this in turn is reflected in their lower melting points. On the other hand, the methyl-group rotation in the *tert*-butyl ester is expected to start *before* the melting onset, leading to a decrease in the ΔS_m term and a concomitant increase in the melting temperature. Stronger or weaker C—H···O interactions do not necessarily lead to more difficult or more easy methyl-group rotations. Perhaps the onset of rotation begins slightly earlier if the interactions are weak, but this has nothing to do with the ease and extent of the free rotation itself which depends on molecular symmetry. It would seem that in D*t*BO, the interactions are strong *and* the free rotation is facile. Therefore, the melting temperature of D*t*BO (343 K) is elevated because of a large value of the ΔH_m term (good interactions) *and* also a small value of the ΔS_m term (rotation of the methyl groups before melting).

4. Conclusions

We may draw the following conclusions based on the original aims of this work:

(i) The high melting points of DMO (327 K) and D*t*BO (343 K) are due to strong and attractive C—H···O hydrogen bonds in these structures. The latter melting point is higher than the former possibly because of entropic reasons.

(ii) Molecules of DEO and D*t*BO occupy general positions in a crystal that takes a centrosymmetric space group. The reason for this is unclear for DEO. For D*t*BO it could be because a good supramolecular synthon lies on the special position.

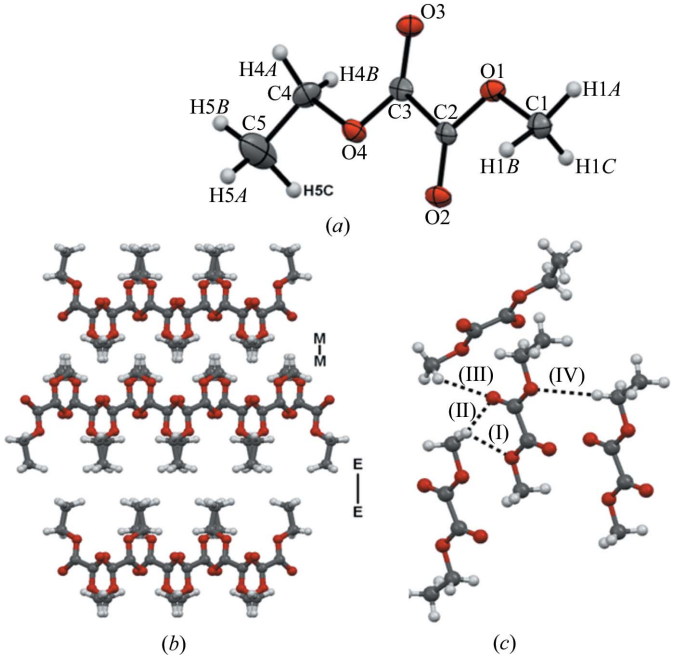

Figure 6
Methyl ethyl oxalate, MEO: (*a*) single molecule *ORTEP* drawing at the 50% probablity level; (*b*) view down the *c* axis to show the layer structure; (*c*) four intermolecular C—H···O interactions observed.

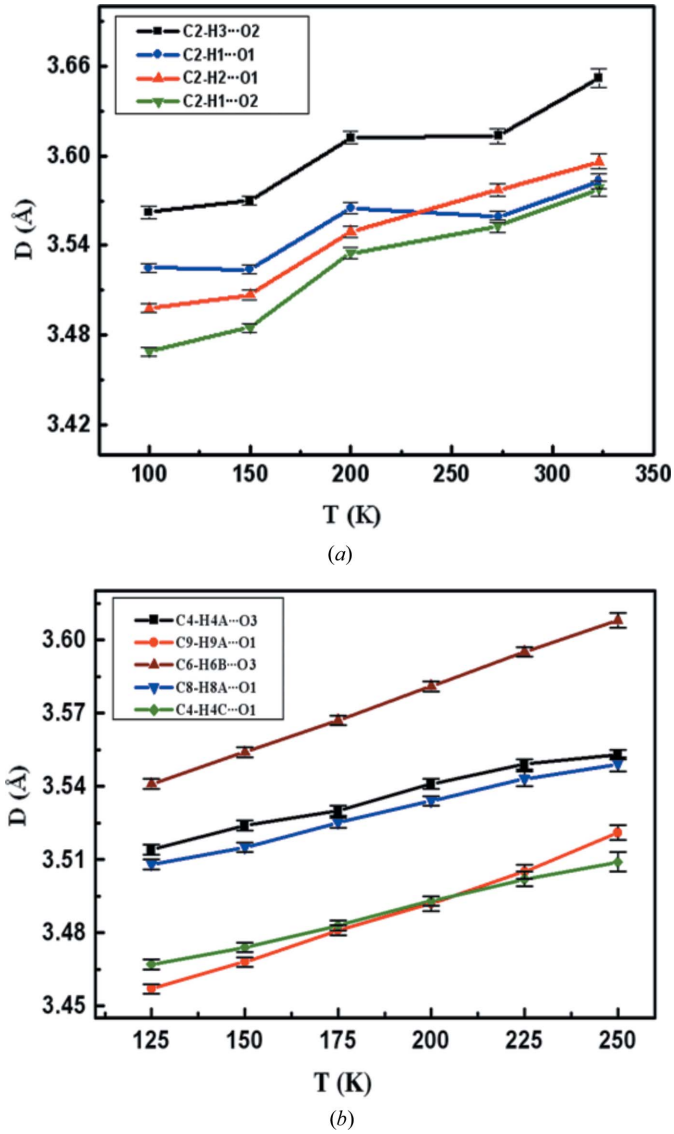

Figure 7
C···O distance (*D*) *versus* temperature for (*a*) DMO and (*b*) D*t*BO showing increased attractive interaction with decreasing temperature.

The crystal structures of the lower aliphatic esters are, not unexpectedly, governed by the orientational preferences of the various C—H···O hydrogen bonds present. Both carbonyl and alkoxyl O atoms are involved with the former being a better acceptor. Hydrogen bonds formed by more activated C—H donors are shorter and more linear. These bonds are of an attractive type, and this is verified with variable-temperature X-ray measurements. Finally, cryocrystallography is becoming an increasingly important tool in the hands of crystal engineers because it draws together a number of compounds that have hitherto been beyond the scope of single-crystal X-ray crystallography. The analysis of single-crystal data for compounds that are liquids at room temperature by a large number of non-specialist crystallographers is a development of importance in structural chemistry.

S. J thanks UGC (GOI) for the award of a D. S. Kothari Postdoctoral Fellowship and G. R. D. thanks DST for the award of a J. C. Bose Fellowship. We thank Rigaku Corporation, Tokyo for their support through a generous loan of a RigakuMercury-375R/M CCD (XtaLAB mini) table-top diffractometer. We thank Professor K. R. Prasad, Indian Institute of Science and Dr D. B. Ramachary, University of Hyderabad for their kind gift of MEO (KRP) and D*i*PO and D*n*BO (DBR).

References

Abramowitz, R. & Yalkowsky, S. H. (1990). *Pharm. Res.* **7**, 942–947.
Altomare, A., Cascarano, G., Giacovazzo, C. & Guagliardi, A. (1993). *J. Appl. Cryst.* **26**, 343–350.
Arunan, E., Desiraju, G. R., Klein, R. A., Sadlej, J., Scheiner, S., Alkorta, I., Clary, D. C., Crabtree, R. H., Dannenberg, J. J., Hobza, P., Kjaergaard, H. G., Legon, A. C., Mennucci, B. & Nesbitt, D. J. (2011*a*). *Pure Appl. Chem.* **83**, 1619–1636.
Arunan, E., Desiraju, G. R., Klein, R. A., Sadlej, J., Scheiner, S., Alkorta, I., Clary, D. C., Crabtree, R. H., Dannenberg, J. J., Hobza, P., Kjaergaard, H. G., Legon, A. C., Mennucci, B. & Nesbitt, D. J. (2011*b*). *Pure Appl. Chem.* **83**, 1637–1641.
Banerjee, R., Desiraju, G. R., Mondal, R., Batsanov, A. S., Broder, C. K. & Howard, J. A. K. (2003). *Helv. Chim. Acta*, **86**, 1339–1351.
Barrow, M. J., Cradock, S., Ebsworth, E. A. V. & Rankin, D. W. H. (1981). *J. Chem. Soc. Dalton Trans.* pp. 1988–1993.
Bock, H., Dienelt, R., Schödel, H. & Havlas, Z. (1993). *J. Chem. Soc. Chem. Commun.* pp. 1792–1793.
Bruker (2004). *SMART* and *RLATT*. Bruker AXS Inc., Madison, Wisconsin, USA.
Derewenda, Z. S., Lee, L. & Derewenda, U. (1995). *J. Mol. Biol.* **252**, 248–262.
Desiraju, G. R. (1991). *Acc. Chem. Res.* **24**, 290–296.
Desiraju, G. R. (2005). *Chem. Commun.* pp. 2995–3001.
Desiraju, G. R. (2011). *Angew. Chem.* **50**, 52–59.
Desiraju, G. R. & Steiner, T. (1998). *The Weak Hydrogen Bond in Structural Chemistry and Biology*. Oxford University Press.
Dougill, M. W. & Jeffrey, G. A. (1953). *Acta Cryst.* **6**, 831–837.
Farrugia, L. J. (1999). *J. Appl. Cryst.* **32**, 837–838.
Jacobson, R. (1998) Private communication.
Jiang, L. & Lai, L. (2002). *J. Biol. Chem.* **277**, 37732–37740.
Jones, G. P., Cornell, B. A., Horn, E. & Tiekink, E. R. T. (1989). *J. Crystallogr. Spectrosc. Res.* **19**, 715–723.
Oxford Diffraction Ltd (2007). *Xcalibur CCD system, CrysAlisPro Software System*, Version 1. 171.32. Oxford Diffraction Ltd, Abingdon, England.
Pflugrath, J. W. (1999). *Acta Cryst.* D**55**, 1718–1725.
Rigaku Corporation (2007). *CrystalClear* 2.0. Rigaku Corporation, Tokyo, Japan.
Scheiner, S., Kar, T. & Gu, Y. (2001). *J. Biol. Chem.* **276**, 9832–9837.
Seiler, P., Isaacs, L. & Diederich, F. (1996). *Helv. Chim. Acta*, **79**, 1047–1058.
Shallard-Brown, H. A., Watkin, D. J. & Cowley, A. R. (2005*a*). *Acta Cryst.* E**61**, o561–o562.
Shallard-Brown, H. A., Watkin, D. J. & Cowley, A. R. (2005*b*). *Acta Cryst.* E**61**, o1118–o1120.
Sheldrick, G. M. (2008). *Acta Cryst.* A**64**, 112–122.
Steiner, T. & Desiraju, G. R. (1998). *Chem. Commun.* pp. 891–892.
Taylor, R. & Kennard, O. (1982). *J. Am. Chem. Soc.* **104**, 5063–5070.
Wahl, M. C. & Sundaralingam, M. (1997). *Trends Biochem. Sci.* **22**, 97–102.